Nighttime chemistry and morning isoprene can drive urban ozone downwind of a major deciduous forest

Dylan B. Millet[*,†], Munkhbayar Baasandorj[†,1], Lu Hu[†,2], Dhruv Mitroo[‡], Jay Turner[‡] and Brent J. Williams[‡]

[†]University of Minnesota, St. Paul MN, USA.

[‡]Washington University in St. Louis, St. Louis MO, USA.

[1]Present address: Utah Department of Environmental Quality, Salt Lake City UT, USA.

[2]Present address: Harvard University, Cambridge MA, USA.

[*] Corresponding author.

Address: University of Minnesota
1991 Upper Buford Circle
St. Paul MN 55108
USA

Tel/Fax: 612-626-3259

Email: dbm@umn.edu

Running title: Nighttime isoprene and morning ozone

SUPPORTING INFORMATION

Contains: 17 pages. Sections S1-S2, Figures S1-S6, References.

S1. Potential Measurement Interferences for Isoprene and MVK+MACR.

As discussed below, we do not expect any measurement interferences for isoprene or MVK+MACR to affect the analyses shown here.

While isoprene hydroxyhydroperoxides (ISOPOOH; produced from OH-driven isoprene oxidation at low NO) can cause interferences with PTR-MS measurements at *m*/*z* 71,[1,2] such compounds are unlikely to affect our analysis or the results shown in Figures 3 and S6. This is the case for several reasons: *i*) The study took place in a clearly high-NO_x environment; isoprene oxidation products produced in the vicinity of the city would not have any important contribution from the ISOPOOH-generating hydroperoxyl pathway. *ii*) Any ambient ISOPOOH would thus have to be transported from the more pristine conditions deep within the Ozarks. However, such compounds are substantially more reactive towards OH than MVK and MACR (with yield-weighted mean rate coefficient 4× the mean of MVK and MACR, based on Ref. 3) and also undergo photolysis. Hence they would be less liable than MVK+MACR to survive transit to the SLAQRS site. *iii*) For ISOPOOH that is transported to the SLAQRS field site, the reported detection efficiency at *m*/*z* 71 is less than half that of MVK and MACR.[2] *iv*) Most importantly, if some of the ambient *m*/*z* 71 signal were ISOPOOH, this would not have an appreciable effect on the predicted trend shown in Figures 3 and S6. The production term (as MVK+MACR) would be computed exactly as before. Like MVK and MACR, ISOPOOH is likely to react relatively slowly with O_3 and NO_3.[3] And in any case, the predicted trend for MVK+MACR is dominated by the mixing term (as can be seen from the dashed black line in Figure S6), and our estimate for this would be the same for ISOPOOH as for

MVK+MACR. In the same context, while ISOPOOH may undergo deposition more rapidly than MVK+MACR, this also means that less would have survived transit to the urban area in the first place.

Likewise, any interferences at *m*/*z* 69 and *m*/*z* 71 from anthropogenic VOCs (including, possibly, anthropogenically-sourced isoprene, MVK, or MACR) should also be of negligible importance for the analyses presented here. Based on simultaneous measurements of other species (C_8 and C_9 aromatics), and following the approach of Hu et al.,[4] we estimate that the median anthropogenic contribution to *m*/*z* 69 and 71 during August and September was < 150 ppt.

S2. Attributing Nighttime Trends in Isoprene and MVK+MACR.

For nights featuring distinct periods with declining isoprene concentrations, we calculate the expected change in isoprene and MVK+MACR over the same period due to O_3, NO_3, and atmospheric mixing as shown in Figures 3 and S6. Chemical loss of isoprene and MVK+MACR due to ozonolysis is computed from measured O_3 and IUPAC-recommended rate coefficients of $k_{298} = 1.27\times10^{-17}$ cm^3 molec^{-1} s^{-1} for isoprene and $k_{298} = 3.2\times10^{-18}$ cm^3 molec^{-1} s^{-1} for MVK+MACR (i.e. the mean of their individual rates).[5] Production of MVK and MACR from isoprene ozonolysis is then estimated from their expected molar yields (0.244 and 0.325, respectively) based on the current GEOS-Chem mechanism.[6] NO_3 was not measured during SLAQRS, so we derive here an estimate of its steady-state abundance based on measurements of the key species driving its production and loss (i.e., NO, NO_2, O_3, isoprene).[7] Production of NO_3 is via $NO_2 + O_3$

(k_{298} = 3.5×10^{-17} cm^3 $molec^{-1}$ s^{-1}; Ref. 8) with loss due to reaction with NO (k_{298} = 2.6×10^{-11} cm^3 $molec^{-1}$ s^{-1}; Ref. 8) and isoprene (k_{298} = 7.0×10^{-13} cm^3 $molec^{-1}$ s^{-1}; Ref. 5). By assuming NO_3 loss in this environment is predominantly via reaction with NO and isoprene, we neglect its indirect loss via heterogeneous uptake of N_2O_5. The NO_3 lifetime due to reaction with NO and isoprene averages $\leq$ 20 s for each of the time periods examined here; on such short time scales NO_3 variability should be dominated by its production and gas phase loss processes.[9] Loss of isoprene and MVK+MACR due to reaction with NO_3 is computed as above for O_3, with k_{298} = 2.0×10^{-15} cm^3 $molec^{-1}$ s^{-1} applied to the sum of MVK and MACR[5] and a 3.5 mol% yield for each of MVK and MACR from isoprene + NO_3.[10,11]

The residual isoprene trend after accounting for its estimated chemical loss to O_3 and NO_3 is then attributed to mixing processes, and fit to an exponential to yield an effective dilution frequency (s^{-1}). That same dilution frequency, plus the above chemical production and loss estimates, is then used to derive the MVK+MACR trend that is expected from the inferred nighttime isoprene budget, as an independent test of the overall approach.

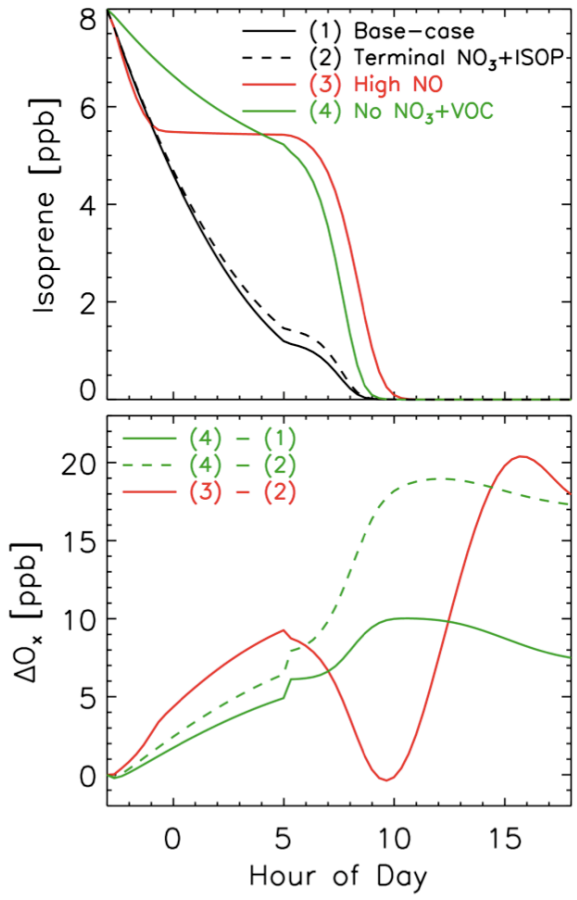

Figure S1. Simulated effects of nighttime isoprene chemistry. Top panel shows isoprene concentrations simulated with the DSMACC chemical box model on nights with lower (0.5 ppb; solid black line) and higher (4 ppb; solid red line) levels of NO. Also shown are sensitivity simulations with *i*) 0.5 ppb NO but no NO_3 + VOC reactions (green) and *ii*) 0.5 ppb NO and isoprene + NO_3 assumed to be a terminal sink for both reactants (i.e., products are lost to deposition or aerosol uptake and do not participate in subsequent gas-phase chemistry; dashed black). The bottom panel shows the resulting O_x (O_3 + NO_2) enhancement over the base-case 0.5 ppb NO simulation for the high-NO case (red) and for the simulation with no NO_3 + VOC reactions (green). Also shown (dashed green) is the O_x enhancement for the same simulation with no NO_3 + VOC reactions but relative to a base-case with terminal isoprene + NO_3 reaction (i.e. the dashed black line in the top

panel). Plotting O_x corrects for O_3 titration by NO; corresponding O_3-only plot shown in Figure S2.

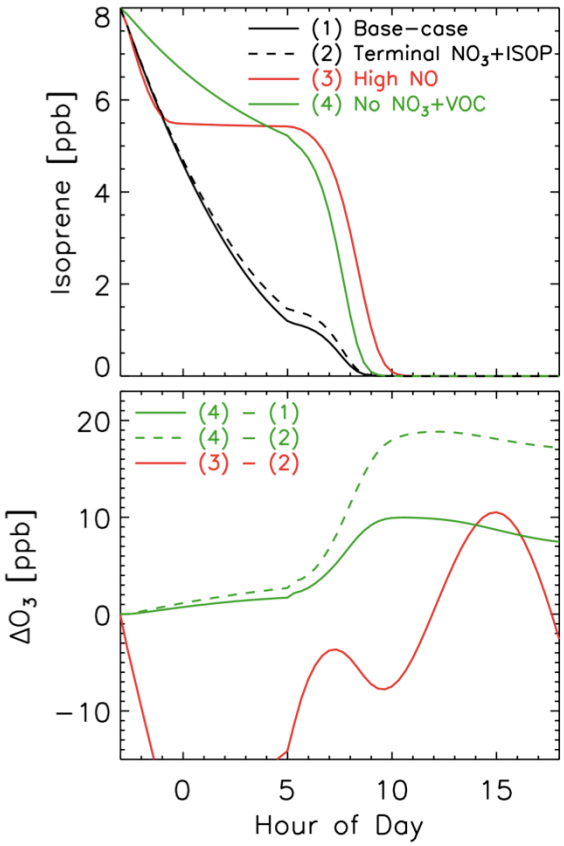

110

111

112 **Figure S2.** Simulated effects of nighttime isoprene chemistry. Same as Figure S1 except

113 showing ΔO_3 rather than ΔO_x.

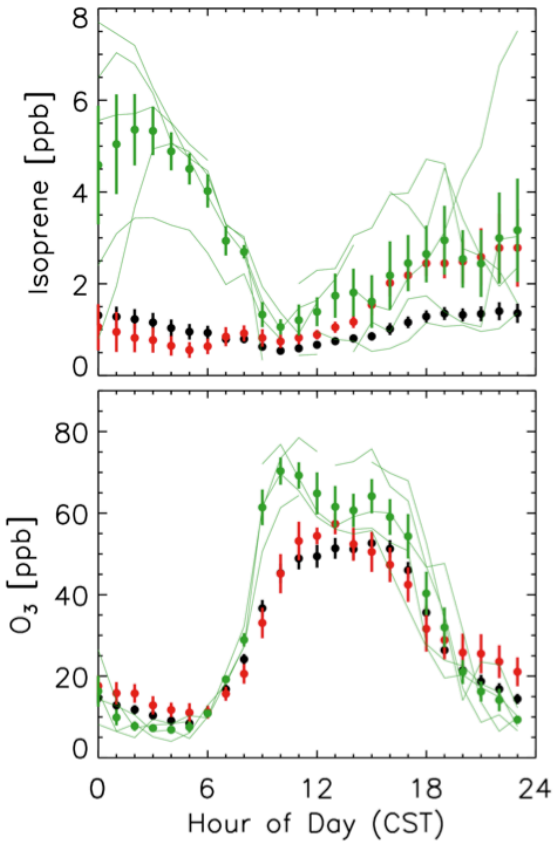

Figure S3. Diurnal cycle in isoprene and O_3 during summer in St. Louis. Shown are the mean observed concentrations by hour for the entire campaign (black) and for days with southwesterly winds (170°-270°) at 06:00 with (green; > 2 ppb) and without (red) elevated isoprene. Error bars show one standard deviation about the mean. Thin green lines show individual days making up the corresponding average. The figure is the same as Figure 4 except here the criterion for southwesterly winds is enforced only at 06:00 rather than throughout the 24-h day. Corresponding O_x (O_3 + NO_2) plot shown in Figure S4.

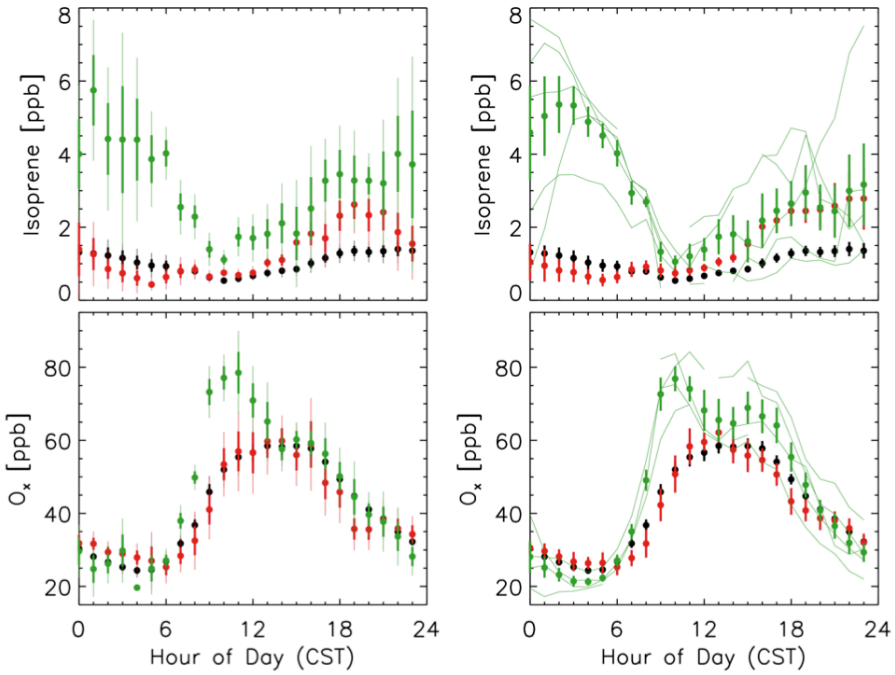

125

126 **Figure S4.** Diurnal cycle in isoprene and O_x (O_3 + NO_2) during summer in St. Louis.

127 Same as Figures 4 (left column) and S3 (right column) except showing O_x rather than O_3,

128 which corrects for O_3 titration by NO.

129

130

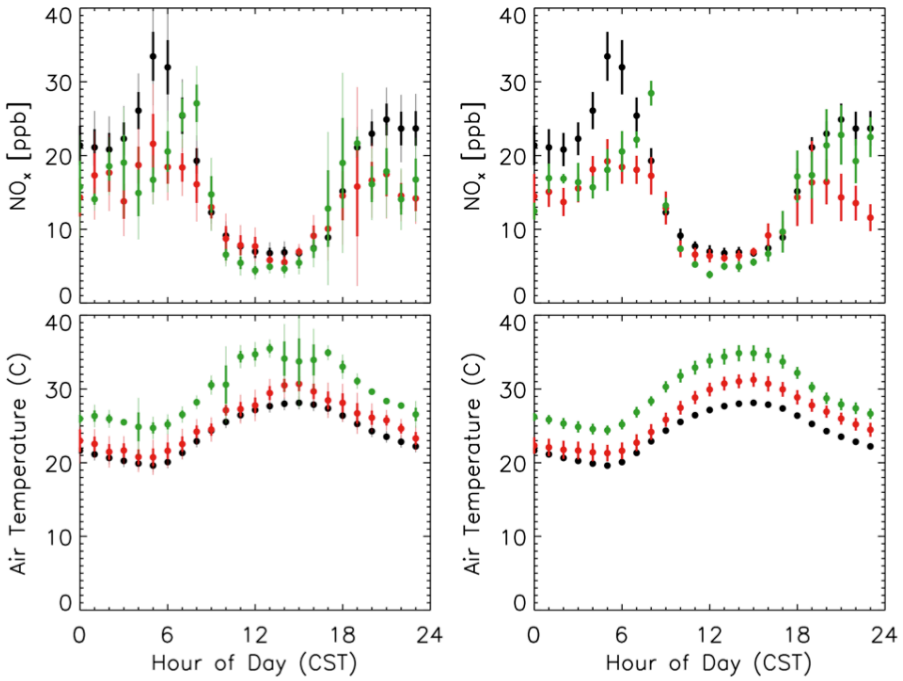

Figure S5. Diurnal cycle in NO_x and in air temperature. Mean hourly values are shown for the entire campaign (black) and for days with southwesterly winds with (green; > 2 ppb at 06:00) and without (red) elevated morning isoprene. The left and right columns show results derived using the averaging strategies of Figures 4 and S3, respectively.

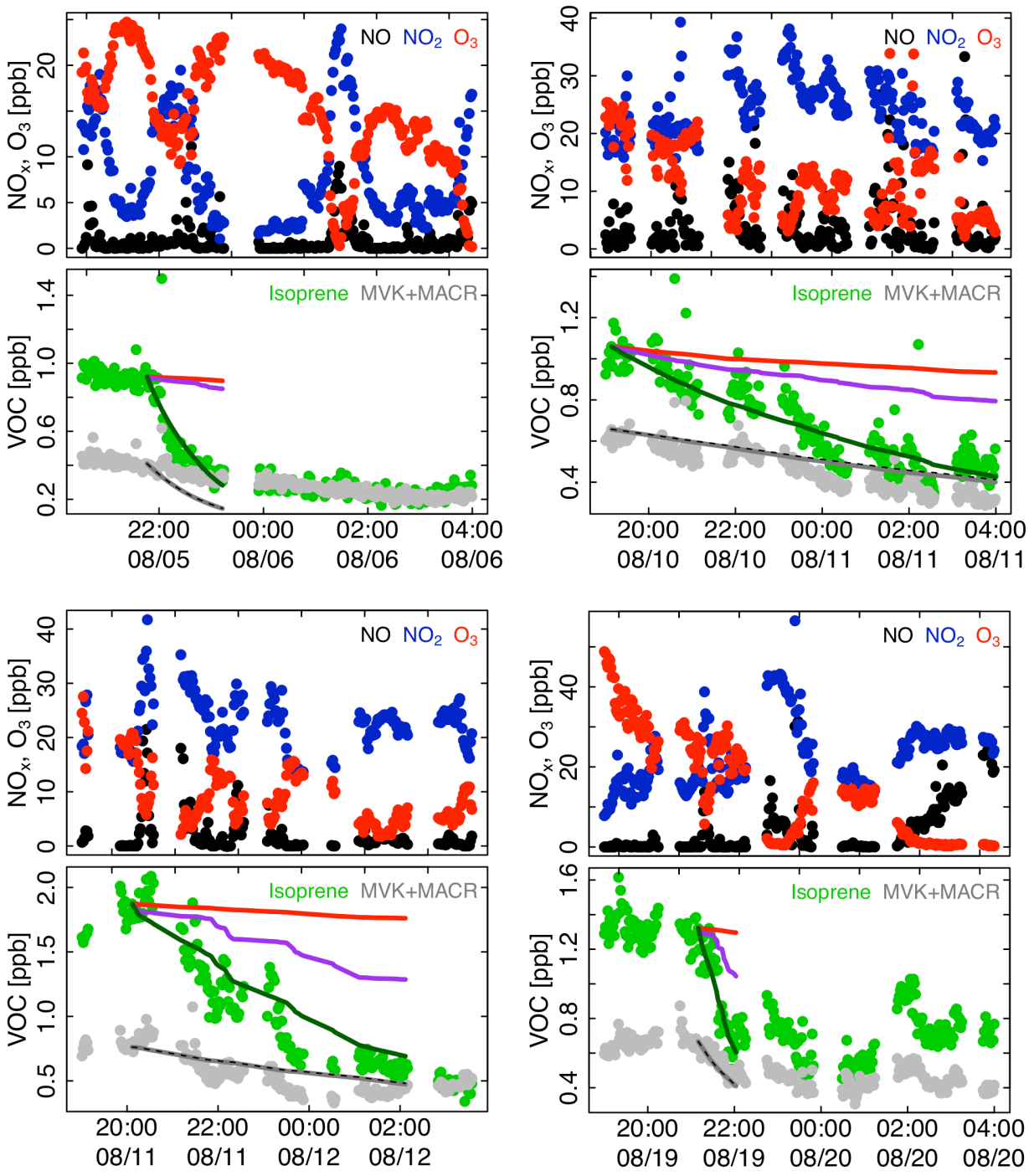

Figure S6. Nighttime isoprene removal. Shown are measurements of NO_x, O_3, isoprene and MVK+MACR for nights with a clearly defined decline in isoprene after dark. Solid lines show the calculated isoprene decay due to O_3 (red), O_3 + NO_3 (purple), and O_3 +

143 NO_3 + mixing (green) as described in-text. Grey lines show the resulting predictions for
144 MVK+MACR. Dashed black lines show the predictions for MVK+MACR based solely
145 on atmospheric mixing.
146
147

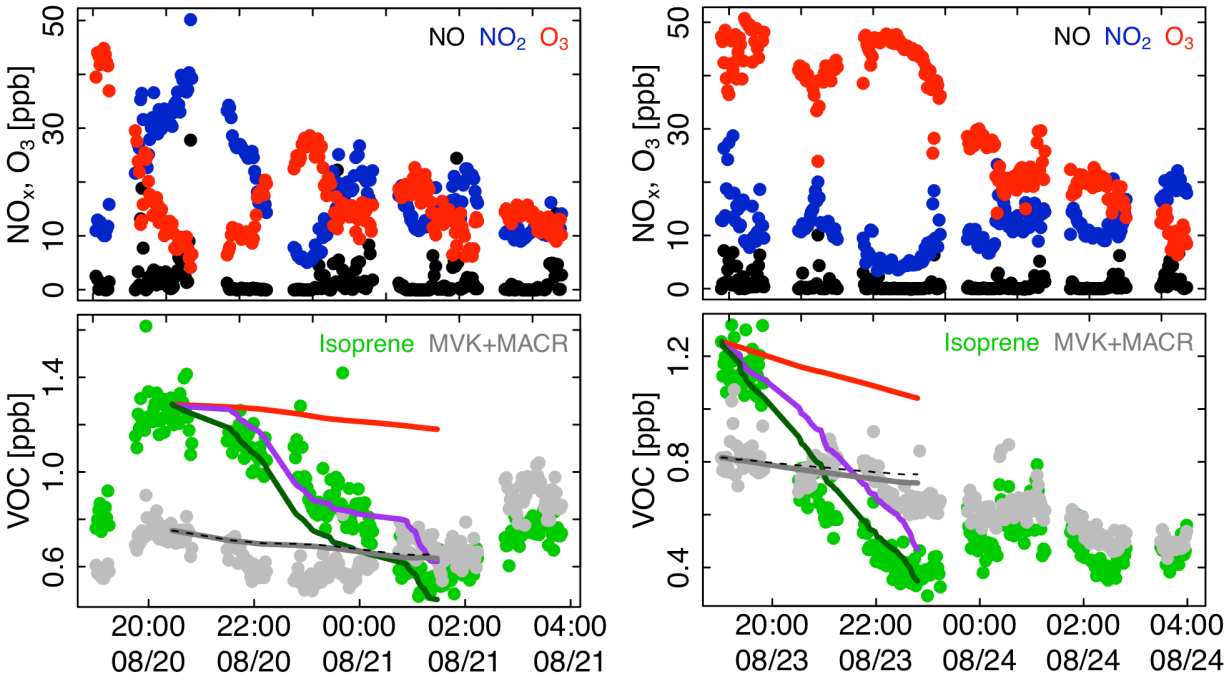

148

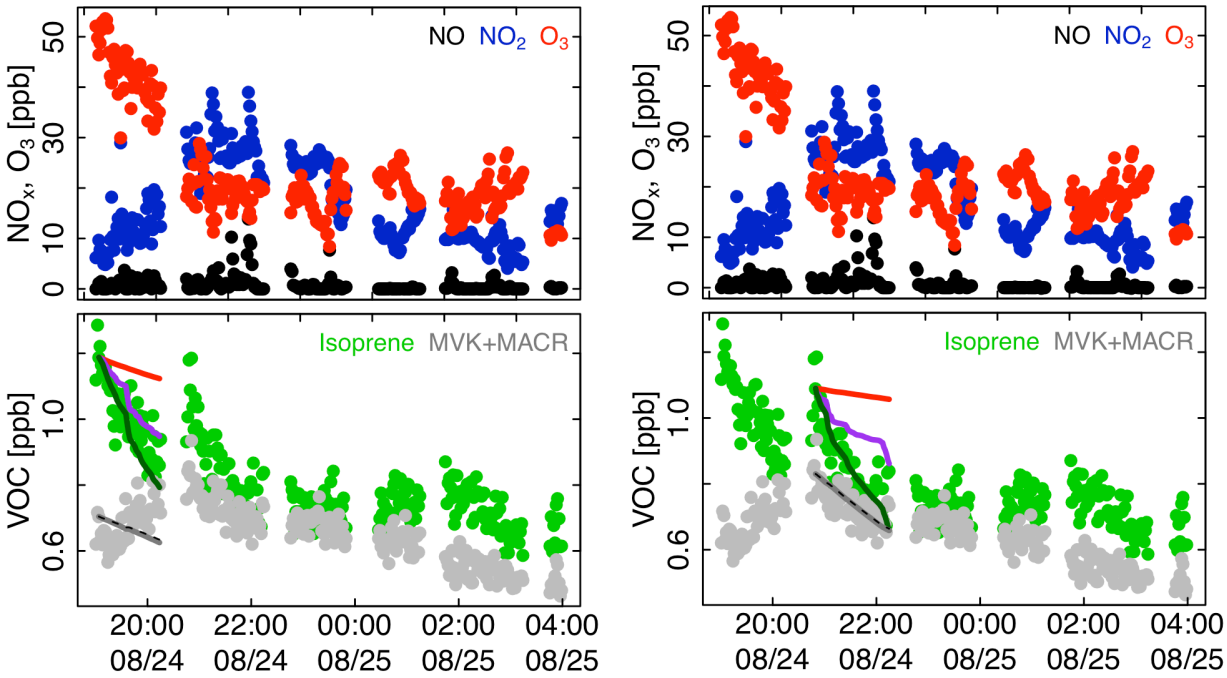

149

150 **Figure S6 (continued).**

151

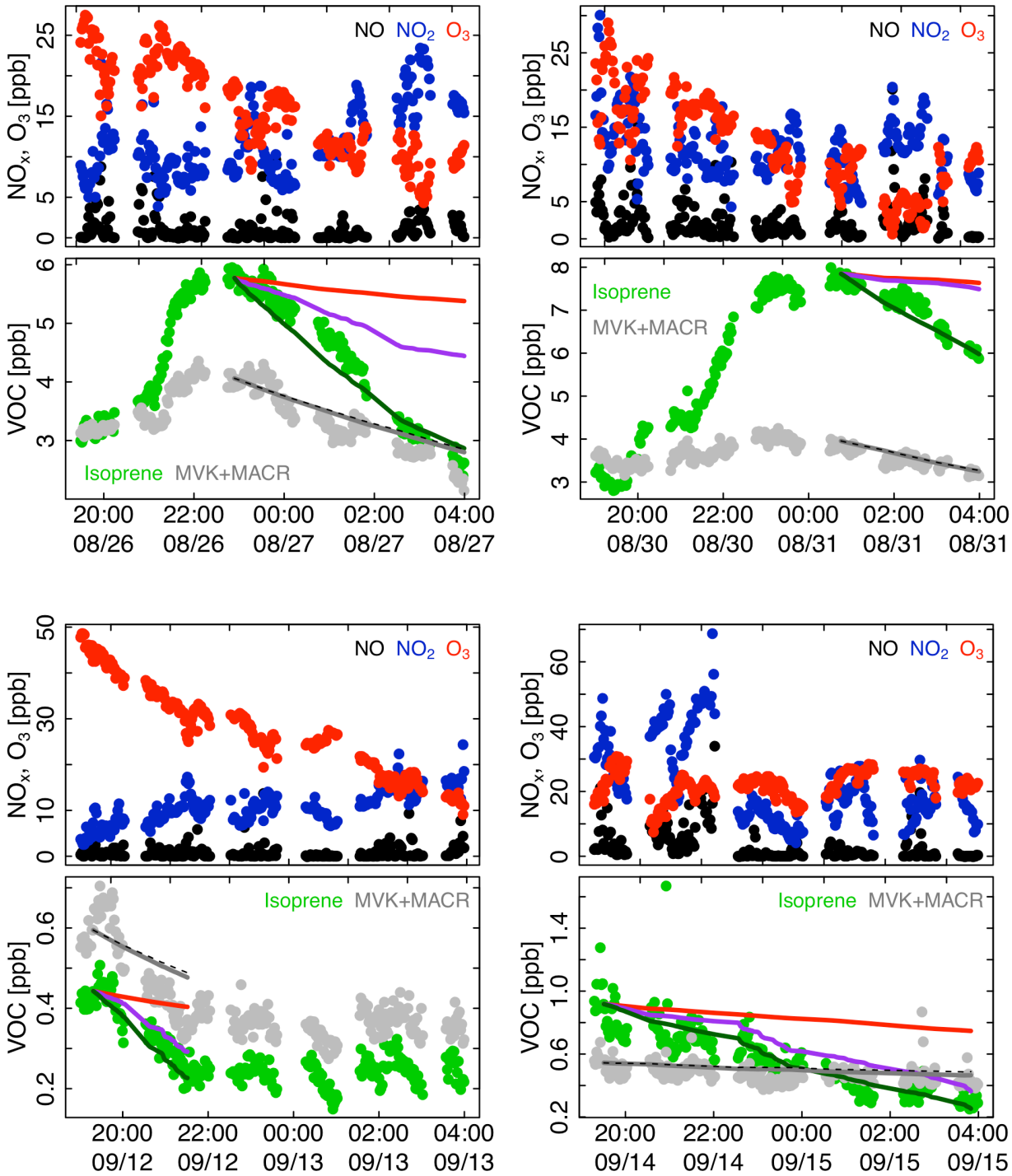

Figure S6 (continued).

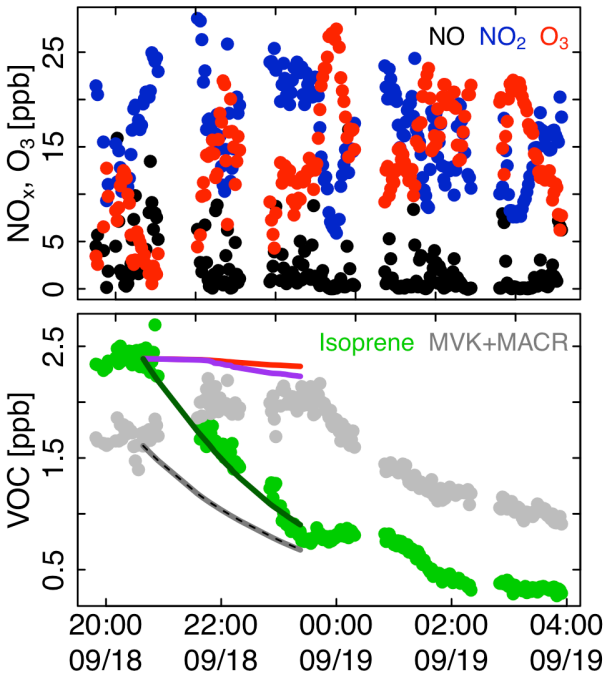

157

158 **Figure S6 (continued).**

159

REFERENCES

(1) Liu, Y.J.; Herdlinger-Blatt, I.; McKinney, K.A.; Martin, S.T. Production of methyl vinyl ketone and methacrolein via the hydroperoxyl pathway of isoprene oxidation. *Atmos. Chem. Phys.* **2013**, *13* (11), 5715-5730; doi:10.5194/acp-13-5715-2013.

(2) Rivera-Rios, J.C.; Nguyen, T.B.; Crounse, J.D.; Jud, W.; St Clair, J.M.; Mikoviny, T.; Gilman, J.B.; Lerner, B.M.; Kaiser, J.B.; de Gouw, J.; Wisthaler, A.; Hansel, A.; Wennberg, P.O.; Seinfeld, J.H.; Keutsch, F.N. Conversion of hydroperoxides to carbonyls in field and laboratory instrumentation: Observational bias in diagnosing pristine versus anthropogenically controlled atmospheric chemistry. *Geophys. Res. Lett.* **2014**, *41* (23), 8645-8651; doi:10.1002/2014gl061919.

(3) Jenkin, M.E.; Young, J.C.; Rickard, A.R. The MCM v3.3.1 degradation scheme for isoprene. *Atmos. Chem. Phys.* **2015**, *15*, 11433-11459; doi:10.5194/acp-15-11433-2015.

(4) Hu, L.; Millet, D.B.; Baasandorj, M.; Griffis, T.J.; Turner, P.; Helmig, D.; Curtis, A.J.; Hueber, J. Isoprene emissions and impacts over an ecological transition region in the US Upper Midwest inferred from tall tower measurements. *J. Geophys. Res.* **2015**, *120*, 3553-3571, doi:10.1002/2014JD022732.

(5) Atkinson, R.; Baulch, D.L.; Cox, R.A.; Crowley, J.N.; Hampson, R.F.; Hynes, R.G.; Jenkin, M.E.; Rossi, M.J.; Troe, J. Evaluated kinetic and photochemical data for atmospheric chemistry: Volume II - gas phase reactions of organic species. *Atmos. Chem. Phys.* **2006**, *6* (11), 3625-4055; doi:10.5194/acp-6-3625-2006.

(6) Mao, J.; Paulot, F.; Jacob, D.J.; Cohen, R.C.; Crounse, J.D.; Wennberg, P.O.; Keller, C.A.; Hudman, R.C.; Barkley, M.P.; Horowitz, L.W. Ozone and organic nitrates over the eastern United States: Sensitivity to isoprene chemistry. *J. Geophys. Res.* **2013**, *118*, 11256–11268, doi:10.1002/jgrd.50817.

(7) Brown, S.S.; Degouw, J.A.; Warneke, C.; Ryerson, T.B.; Dube, W.P.; Atlas, E.; Weber, R.J.; Peltier, R.E.; Neuman, J.A.; Roberts, J.M.; Swanson, A.; Flocke, F.; McKeen, S.A.; Brioude, J.; Sommariva, R.; Trainer, M.; Fehsenfeld, F.C.; Ravishankara, A.R. Nocturnal isoprene oxidation over the Northeast United States in summer and its impact on reactive nitrogen partitioning and secondary organic aerosol. *Atmos. Chem. Phys.* **2009**, *9* (9), 3027-3042; doi:10.5194/acp-9-3027-2009.

(8) Atkinson, R.; Baulch, D.L.; Cox, R.A.; Crowley, J.N.; Hampson, R.F.; Hynes, R.G.; Jenkin, M.E.; Rossi, M.J.; Troe, J. Evaluated kinetic and photochemical data for atmospheric chemistry: Volume I - gas phase reactions of O_x, HO_x, NO_x and SO_x species. *Atmos. Chem. Phys.* **2004**, *4*, 1461-1738; doi:10.5194/acp-4-1461-2004.

(9) Martinez, M.; Perner, D.; Hackenthal, E.M.; Kulzer, S.; Schutz, L. NO_3 at Helgoland during the NORDEX campaign in October 1996. *J. Geophys. Res.* **2000**, *105* (D18), 22685-22695; doi:10.1029/2000jd900255.

(10) Kwok, E.S.C.; Aschmann, S.M.; Arey, J.; Atkinson, R. Product formation from the reaction of the NO_3 radical with isoprene and rate constants for the reactions of methacrolein and methyl vinyl ketone with the NO_3 radical. *Int. J. Chem. Kinet.* **1996**, *28* (12), 925-934.

(11) Brown, S.S.; Stutz, J. Nighttime radical observations and chemistry. *Chem. Soc. Rev.* **2012**, *41* (19), 6405-6447; doi:10.1039/c2cs35181a.